

## COMPARATIVE EFFECTIVENESS OF INTRAPERITONEAL AND INTRAMUSCULAR <sup>3</sup>H-TDR INJECTION ROUTES IN MICE<sup>1</sup>

M. R. SKOUGAARD<sup>2</sup> and P. A. STEWART<sup>3</sup>

*Biology Department, Brookhaven National Laboratory, Upton, N.Y. 11973, U.S.A.*

Received August 8, 1966

In tritiated thymidine (<sup>3</sup>H-TDR) autoradiography, intraperitoneal injection of label is very frequently used, especially in small animals. The kinetics of the numerous processes involved between injection and incorporation into nuclear DNA are not well established, however. Recent work on the marmoset [14] has shown that only a small fraction of the injected <sup>3</sup>H-TDR is incorporated into DNA, and that the yield of autoradiographic grain counts depends on the time course of tracer concentration in the bloodstream. <sup>3</sup>H-TDR is a major part of the nonvolatile <sup>3</sup>H-plasma activity only during the first few minutes after injection. Significantly different results were obtained when intramuscular (IM) rather than intraperitoneal (IP) injection was used. The four-factor model introduced by Quastler [9] predicts such results, but has been tested in detail only for IP injection in the mouse [17].

The kinetics of thymidine incorporation into DNA after IP injection into mice have also been studied indirectly by a number of workers. On the basis of time taken for maximum crypt cell labeling to occur, Quastler and Sherman [11] concluded that IP injected <sup>3</sup>H-TDR was completely absorbed from the peritoneal cavity by 16 min post-injection. Quastler and Kember [10] measured the tritium content of peritoneal washings as a function of time after injection, and concluded that uptake of <sup>3</sup>H-TDR into the circulation followed a double exponential curve with half-times of approximately  $\frac{1}{2}$  min and 5 min. They also found that maximum autoradiographic labeling had occurred in the intestinal crypt cells 15 min after the injection. Staroscik *et al.* [15] found uptake of <sup>3</sup>H-TDR still occurring into mouse mammary

<sup>1</sup> Research carried out at Brookhaven National Laboratory under the auspices of the U.S. Atomic Energy Commission.

<sup>2</sup> Present address: Department of Periodontology, Royal Dental College, Copenhagen, Denmark.

<sup>3</sup> Present address: Division of Medical Science, Brown University, Providence, R.I. 02912, U.S.A.

gland tumors 40 min after injection. They estimated the rate of uptake by evaluating the derivative of the curve of autoradiographic labeling versus time after injection and found a rapid initial phase followed by an exponential curve with a half-time of about 10 min. Bresciani [2] used the derivative of the autoradiographic labeling curve from the same tissue to estimate the activity of <sup>3</sup>H-TDR in the bloodstream. He found an approximately exponential decrease with a half-time of about 7 min. Rubini *et al.* [13] carried out studies of <sup>3</sup>H-activities measured directly in the blood plasma of man following intravenous injection of <sup>3</sup>H-TDR. They found a double exponential disappearance curve with half-times of 0.2 and 6 min.

In the present study, intraperitoneal and intramuscular injection routes for <sup>3</sup>H-TDR in mice have been compared with respect to the following parameters:

(1) Time course of blood plasma activity level of total tritium, volatile tritium, nonvolatile tritium and tritiated thymidine.

(2) Final levels of labeling intensity (mean grains per labeled nucleus) in oral epithelial and intestinal crypt cell autoradiographs.

#### MATERIALS AND METHODS

Ninety-six Walter Reed Hospital Swiss pathogen-free mice from the laboratory colony were used for the experiment [5]. Three- to 4-month-old males from 26 litters, ranging from 27 to 36 g were selected. Tritiated thymidine with a specific activity of 6.5 c/mole was heated to 36°C and injected at a dose of 2  $\mu$ c per g body weight, either IP or IM, into the right thigh muscle mass.

Blood samples were taken at intervals of 1 to 90 min after injection, only one sample being taken from each animal. One-minute samples were obtained by decapitating the animals over a heparinized centrifuge tube. Samples of 0.5 ml were obtained in 3 to 5 sec in this way, but the blood tended to coagulate extremely rapidly. Therefore this technique was only used for the 1-min samples, for which the time factor was critical. The later blood samples were taken by aspiration through a thin heparinized glass pipette inserted behind the eyeball into the infraorbital venous plexus. Samples of 0.5 ml were obtained within 20 to 30 sec by this technique. All samples were immediately sealed, chilled to 4°C and centrifuged 30 min at 3450  $\times$  g. Exposure of samples to air was kept at a minimum to avoid loss of volatile tritium-containing components.

Aliquots of 100  $\mu$ l of plasma were transferred to counting vials and 3.9 ml ethyl alcohol plus 16 ml of 0.3 per cent PBD-xylene added for measurement of total plasma tritium activity. Volatile tritium activity was determined on another 100  $\mu$ l aliquots by distilling the volatile components into a counting vial chilled with dry ice and acetone (Fig. 1). The sample was placed in the small lower vial, which was immediately clamped to the closely-fitting upper vial. The lower vial was then heated in

a boiling water bath while the upper vial was surrounded by the dry ice-acetone freezing mixture. After 5 min the whole unit was disassembled and the upper vial sealed immediately after addition of ethyl alcohol and PBD-xylene.

Test runs with known amounts of tritiated water showed 100 per cent recovery by this technique. All samples were counted in a liquid scintillation spectrometer for a period of time sufficient to reach a minimum of  $10^4$  counts. Background and standard counts were determined for each day of counting, and results corrected accordingly. The efficiency of the scintillation spectrometer was found to be 8 per cent. Nonvolatile tritium activity of plasma was calculated by subtracting volatile activity from total activity as determined from these two aliquots of each sample.

For determinations of the per cent of  $^3\text{H}$ -TDR in the nonvolatile tritium activity, samples of pooled blood from four animals at each specific time were centrifuged. After protein precipitation with trichloroacetic acid, plasma samples were centrifuged at  $3450 \times g$  for 30 min. The supernatant was neutralized to pH 7.0 with 1.0 N NaOH, lyophilized and reconstituted to 200  $\mu\text{l}$  with distilled water. A 10  $\mu\text{l}$  aliquot of this solution was then analyzed by ascending paper chromatography using the upper layer from an ethyl acetate:water:formic acid:60:35:5 mixture [4]. Additional thymidine carrier was added to the sample spot before chromatography. The thymidine spot was identified under ultraviolet light, cut out of the paper, eluted into Bray's solution [1] and counted in the liquid scintillation spectrometer.

The activity of 10  $\mu\text{l}$  of the reconstituted sample was also determined by letting it dry into a spot on filter paper, cutting out this spot, and treating it exactly as the  $^3\text{H}$ -TDR spot was treated. The percentage of  $^3\text{H}$ -TDR in the total nonvolatile plasma tritium activity was then calculated from the ratio of the two counts.

For autoradiography, small pieces of intestine and sublingual tissue were fixed in Carnoy's solution immediately after sacrifice, stained by conventional Feulgen technique and dissected to provide squash preparations of the epithelia on microscope slides. Kodak NTB liquid emulsion was used, and emulsion-covered slides were exposed for appropriate periods of time in the cold, with dessicant [3]. After photographic processing, grains over the nuclei were counted and the resulting data processed by an IBM 7094 computer.<sup>1</sup>

## RESULTS AND DISCUSSION

### *Time course of tritiated components in bloodstream*

The total volatile and nonvolatile (by subtraction) plasma activities are plotted against time in Figs. 2-4. Each point on these curves represent the average value for the 4 mice sacrificed at the indicated time after injection.

In the IP injected mice, total  $^3\text{H}$ -activity reached its maximum value of  $2 \times 10^4$  cpm/100  $\mu\text{l}$  plasma almost immediately following injection, and remained at this level during the rest of the experiment. Volatile  $^3\text{H}$ -activity

<sup>1</sup> The program for the computer was devised by Mr K. Thompson of the Biology Department, Brookhaven National Laboratory.

increased at a slower rate, but eventually reached a plateau level indistinguishable from that of the total activity. The nonvolatile activity, measured as the difference between total and volatile, increased to a maximum and then fell off slowly to negligible values. The form of the curves for the IM

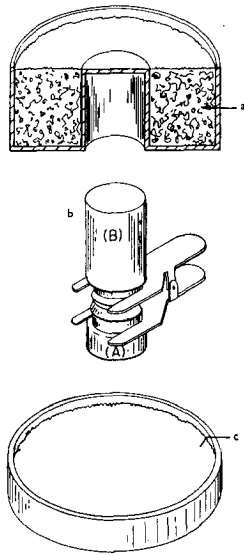


Fig. 1.

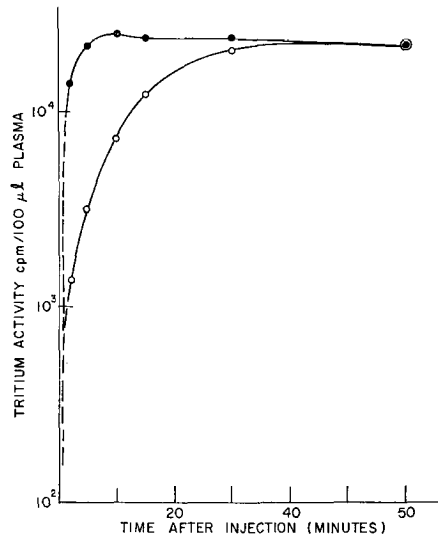


Fig. 2.

Fig. 1.—Device used to collect volatile plasma components in the liquid scintillation counting vial (B). When sealed by the clamp the two vials, A and B, fit closely. a, dry ice acetone; b, vial; c, boiling water.

Fig. 2.—Semilogarithmic graph demonstrating the total and the volatile  $^3\text{H}$ -activities in the blood plasma vs. time after IP injection of  $^3\text{H-TDR}$ . Each point represents the average activity for the 4 mice sacrificed at the time interval in question. ●—●, total plasma  $^3\text{H}$ -activity; ○—○, volatile plasma  $^3\text{H}$ -activity.

injected mice was similar, but all changes were slower. It was possible in this case to observe the increase in total plasma activity during the first 5 min after IM injection, and the rate of disappearance of nonvolatile activity was much less than after IP injection. It is evident from the figures that the decrease in nonvolatile  $^3\text{H}$ -activity was exponential following IP as well as IM injection and dropped to negligible values by 30 min after IP or 60 min after IM injection.

Attempts were made to determine total plasma activity immediately after IP injection. In all cases results on the order of  $2 \times 10^4$  cpm/100  $\mu\text{l}$  plasma were obtained, so that we may take this number as a measure of the initial

total plasma activity. If all the injected  $^3\text{H}$ -TDR ( $2 \mu\text{c/g}$ ) were distributed uniformly over the extracellular water phase, which we take to be 20 per cent of the body weight [6, 16], the expected initial activity would be  $2 \times 10^5$  cpm/100  $\mu\text{l}$  plasma. This suggests that approximately 90 per cent of the IP

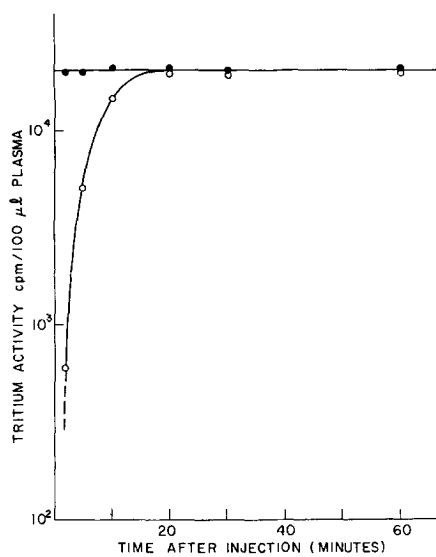


Fig. 3.

Fig. 3.—Semilogarithmic graph demonstrating the total and the volatile  $^3\text{H}$ -activities in the blood plasma vs. time after IM injection of  $^3\text{H}$ -TDR. Each point represents the average activity for the 4 mice sacrificed at the time interval in question. ●—●, Total plasma  $^3\text{H}$ -activity; ○—○, volatile plasma  $^3\text{H}$ -activity.

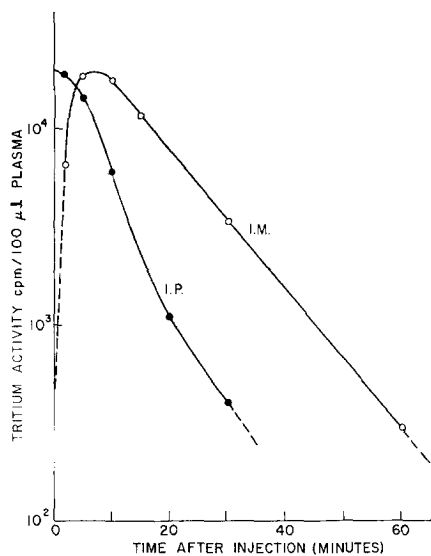


Fig. 4.

Fig. 4.—Semilogarithmic graph showing the nonvolatile  $^3\text{H}$ -activity in the plasma vs. time after IP and IM injections. ●—●, IP injection; ○—○, IM injection.

injected  $^3\text{H}$ -TDR is catabolized, probably via the hepatic portal system and the liver [8] and not released into the systemic circulation.

Results of the paper-chromatographic analysis of the plasma tritium activities are plotted in Fig. 5. The  $^3\text{H}$ -TDR activity constituted a rapidly decreasing percentage of the nonvolatile activity, and decreased more rapidly after IP than after IM injection. This difference might be expected to result from the more direct route to liver catabolic mechanisms from intraperitoneal sites than from intramuscular.

Multiplying the  $^3\text{H}$ -TDR percentages from Fig. 5 by the nonvolatile activities for corresponding times (Fig. 4) gives the actual plasma  $^3\text{H}$ -TDR values expressed as cpm/100  $\mu\text{l}$  plasma. In Fig. 6 these  $^3\text{H}$ -TDR concentrations

# Explore Litigation Insights

Docket Alarm provides insights to develop a more informed litigation strategy and the peace of mind of knowing you're on top of things.

## Real-Time Litigation Alerts



Keep your litigation team up-to-date with **real-time alerts** and advanced team management tools built for the enterprise, all while greatly reducing PACER spend.

Our comprehensive service means we can handle Federal, State, and Administrative courts across the country.

## Advanced Docket Research



With over 230 million records, Docket Alarm's cloud-native docket research platform finds what other services can't. Coverage includes Federal, State, plus PTAB, TTAB, ITC and NLRB decisions, all in one place.

Identify arguments that have been successful in the past with full text, pinpoint searching. Link to case law cited within any court document via Fastcase.

## Analytics At Your Fingertips



Learn what happened the last time a particular judge, opposing counsel or company faced cases similar to yours.

Advanced out-of-the-box PTAB and TTAB analytics are always at your fingertips.

## API

Docket Alarm offers a powerful API (application programming interface) to developers that want to integrate case filings into their apps.

## LAW FIRMS

Build custom dashboards for your attorneys and clients with live data direct from the court.

Automate many repetitive legal tasks like conflict checks, document management, and marketing.

## FINANCIAL INSTITUTIONS

Litigation and bankruptcy checks for companies and debtors.

## E-DISCOVERY AND LEGAL VENDORS

Sync your system to PACER to automate legal marketing.